Electronic structure of warm dense silicon dioxide

K. Engelhorn, V. Recoules, B. Cho, B. Barbrel, S. Mazevet, D. Krol, R. Falcone, P. Heimann

Electronic structure of warm dense silicon dioxide

K. Engelhorn,[1,2,*] V. Recoules,[3] B. I. Cho,[4] B. Barbrel,[5] S. Mazevet,[6] D. M. Krol,[7] R. W. Falcone,[1,5] and P. A. Heimann[8,†]

[1]*Advanced Light Source, Lawrence Berkeley National Laboratory, Berkeley, California 94720, USA*

[2]*Department of Applied Science and Technology, UC Berkeley, California 94720, USA*

[3]*CEA, DAM, DIF, F-91297 Arpajon, France*

[4]*Department of Physics and Photon Science, Gwangju Institute of Science and Technology, Gwangju, Korea*

[5]*Department of Physics, UC Berkeley, Berkeley, California 94720, USA*

[6]*LUTH, Observatoire de Paris, Paris, France*

[7]*Department of Chemical Engineering and Materials Science, UC Davis, Davis, California 95616, USA*

[8]*Linac Coherent Light Source, SLAC National Accelerator Laboratory, Menlo Park, California 94025, USA*

(Received 13 August 2014; revised manuscript received 19 May 2015; published 17 June 2015)

The electronic structure of warm dense silicon dioxide has been investigated by x-ray absorption near-edge spectroscopy. An ultrafast optical laser pulse was used to isochorically heat a thin silicon dioxide sample, and measured spectra were compared with simulations generated by molecular dynamics and density functional theory. In comparison with the room temperature spectrum, two features were observed: a peak below the band gap and absorption within the band gap. This behavior was also observed in the simulations. From consideration of the calculated spectra, the peak below the gap is attributed to valence electrons that have been promoted to the conduction band, while absorption within the gap is attributed to broken Si-O bonds.

DOI: 10.1103/PhysRevB.91.214305 PACS number(s): 71.22.+i, 52.50.Jm, 78.70.Dm, 79.20.Ds

Warm and dense matter may be defined by temperatures of $\sim 10^4 - 10^5$ K and near solid densities [1]. The theoretical description under such conditions is difficult because it falls between the traditional and well understood density and temperature phase space of plasma physics and condensed matter. The study of materials in the warm dense matter regime has implications for planetary interiors [2] and inertial confinement fusion [3].

Silicon dioxide is a major constituent of the earth's crust and mantle. It is also a common material for optics, and optical damage can be initiated at "warm" conditions caused by the laser-matter interaction at high intensities. Additionally, optical waveguides have been written in fused silica by intense femtosecond optical pulses [4]. The mechanism is understood to involve the formation of a localized plasma followed by a microexplosion inside the glass. Specifically at fluences below 8 J/cm^2, smooth waveguides are formed, while at higher fluence rough waveguides are produced. From *ex situ* Raman scattering measurements, an increase in three- and four-membered rings in the silica network is inferred to be the result of the high intensity interaction. As illustrated by the work reported here, ultrafast spectroscopy of transient warm dense silicon dioxide could provide information about the electronic and ionic states underlying the mechanisms of optical damage and waveguide writing by femtosecond lasers.

X-ray absorption near-edge spectroscopy (XANES) probes the unoccupied electronic density of states (DOS). This technique has been applied to studies of warm dense aluminum [5–7], iron [8,9], and copper [10]. In aluminum, a broadening of the K edge and a smoothing of the aluminum absorption spectrum were observed as the solid sample becomes a liquid and then a plasma. By comparing the experimental spectra with *ab intio* calculations, it was shown that the slope of the absorption edge was connected to the electron distribution function and temperature, and the broadening of the structure above the edge was correlated with a loss of order in the high temperature liquid. In the case of aluminum, either heated by protons or compressed by a shock, electron-ion equilibrium was assumed ($T_e = T_i$) because the relative time scales were tens of picoseconds. On the other hand, heating with an ultrafast ($\sim$100 fs) optical pulse results in a nonequilibrium condition, $T_e > T_i$. In aluminum, short range disordering was observed following the laser pulse [7]. From the XANES spectrum of warm dense copper, temperatures of about 1 eV were determined, and the electron-phonon coupling could be inferred from the temporal evolution of the electron temperature [10]. Electron-phonon coupling has also been extensively modeled in metals [11], and measured in proton heated carbon [12] and shock compressed silicon [13]. Electron-phonon coupling is dependent on the details of the electronic structure and vibrational spectrum. It can vary by two orders of magnitude, resulting in electron-ion equilibration times of warm dense matter from a few picoseconds in the case of copper to 100 ps for carbon.

In SiO_2 previous electron spin resonance experiments have shown that ultrafast laser pulses can induce E' center defects [14]. In an E' center, a Si atom is bonded to three oxygen atoms with a dangling sp^3 orbital. Using *ab initio* molecular dynamics (MD) simulations, Boero *et al.* [15] modeled the femtosecond laser irradiation by considering initial conditions of high T_e and ambient T_i. At 25 000 K T_e, Si-Si bonds were observed and displaced O atoms appear in three-membered rings.

Most recently, Denoeud *et al.* [16] used silicon K-edge XANES to study shock compressed SiO_2 at $1-5$ g/cm^3 and temperatures up to 5 eV. DFT calculations agreed well with the measured spectra and indicated a pseudogap corresponding to either a semimetal or a significant metallic component of warm dense SiO_2. The pseudogap was associated with a loss of Si and O correlation.

*kce@berkeley.edu

†paheim@slac.stanford.edu

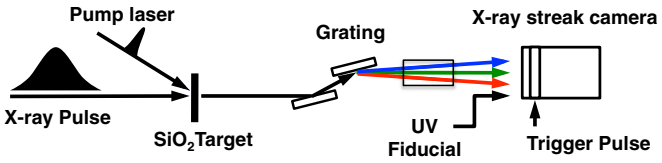

FIG. 1. (Color online) The experimental setup at the Advanced Light Source Beamline 6.0.2.

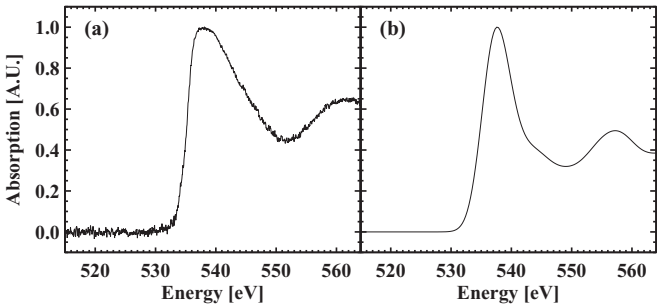

FIG. 2. The experimental and calculated O 1*s* XANES spectrum of SiO_2 at room temperature [(a) and (b)].

Here we present a study of the electronic structure of warm dense silicon dioxide created by ultrafast laser excitation and probed by time-resolved XANES. MD and DFT simulations are used to support the interpretation of the experimental spectra. This leads to conclusions about the modification of bonding following an ultrafast laser excitation.

The experiments were performed at Beamline 6.0.2 at the Advanced Light Source synchrotron facility at Lawrence Berkeley National Laboratory. The experimental setup is shown in Fig. 1. The sample is 400 nm thick amorphous SiO_2. The sample is deposited from crystalline material via *e*-beam evaporation to a room temperature substrate, resulting in an amorphous structure [17]. The sample is then attached to a supporting mesh. A 150 fs, ∼10 mJ Ti:sapphire laser pulse is focused to a 250 or 400 μm (FWHM) diameter spot at the sample depending on the required fluence. Silicon dioxide is an insulator whose band gap, in both amorphous and crystalline phases, is 8.9 eV [18,19]. This greatly exceeds the energy of the optical photons, 1.5 eV. The absorption of the optical photons occurs through multiphoton absorption exciting electrons from the valence band to the conduction band, free carrier absorption of electrons once in the valence band, and plasma absorption after the conduction electrons reach a density approaching the critical density n_c [20]. At the beginning of the laser pulse multiphoton absorption is expected to predominate, while at the end of the pulse, interaction with the plasma should be most important. The optical absorption of the sample was measured at 800 nm by using an integrating sphere to collect the reflected and transmitted portions of the laser beam. The absorption was observed to increase roughly linearly from 6% at low fluence (2.5 J/cm^2) to 25% at high fluence (15 J/cm^2). It should be noted that the measured absorption is averaged over the temporal and spatial profile of the laser pulse and sample thickness. The excitation of the sample at the front and back surfaces varies according to the optical absorption. Since the sample remains mostly transparent, it is expected to be heated relatively uniformly across its thickness, although there may be increased variation because of the nonlinear absorption mechanisms. The laser intensity also had transverse nonuniformity within the x-ray probe area, this is determined by observing the distribution of laser intensities within the x-ray beam. The absorbed energy densities given below are average values, where σ_+ is 10% above and σ_- is 35% below the stated values.

The SiO_2 sample is probed by a 70 ps duration, polychromatic x-ray pulse tuned to the oxygen *K* edge. The x-ray bandwidth ∼25 eV was limited by the grating dispersion onto the streak camera slit. Consequently three spectral windows with different central photon energies were stitched together to produce the complete spectra shown below. The spectra have been confirmed with lower resolution spectra in which no stitching was preformed. A pair of slits reduces the x-ray spot size to either 150 × 150 μm^2 or 150 × 250 μm^2, in order that an area of relatively uniform fluence is sampled within the laser spot. The x rays transmitted through the sample are dispersed by a variable line spaced grating spectrometer [21] and focused horizontally onto an x-ray streak camera [22]. The XANES spectra have an energy resolution of 0.6 eV determined mainly by the dispersion of the spectrometer and the spatial resolution of the streak camera. The x rays impinge on the streak camera photocathode at a 20 deg angle of incidence, which improves the quantum efficiency with respect to normal incidence. A timing fiducial is provided by a portion of the laser beam, which is frequency tripled in BBO crystals. This fiducial allows for calibration of the time axis and correction of temporal jitter. The time resolution of the streak camera is 2 ps, which is primarily limited by the anode slit width and the secondary electron energy distribution. After each laser pulse the sample is translated to avoid the damaged area created by the previous laser pulse, and single shot spectra are collected at ∼1 Hz. Roughly 100 spectra are averaged for each laser fluence.

Figure 2(a) shows the oxygen *K*-edge XANES spectrum of SiO_2 at room temperature. The oxygen absorption edge is seen at 535 eV as well as two maxima above the edge. The measured spectrum is in agreement with the spectrum of vitreous silica [23]. Compared to the spectrum of α-quartz obtained by electron energy loss spectroscopy and XANES [24,25], the second peak of vitreous silica is observed at lower energy, but the general spectral features are mostly unchanged. This indicates that the XANES spectrum reflects the local structure of oxygen bonding. The spectra do not show the double peak feature characteristic of stishovite built from SiO_6 octahedra [24]. The structure of both α-quartz and vitreous silica is based on SiO_4 tetrahedra connected by corner-shared oxygen atoms. From multiple scattering calculations, Davoli *et al.* [26] concluded that the energy separation between the two peaks is sensitive to the Si-O-Si angle, which effects the local environment of the oxygen atoms [27]. Amorphous SiO_2 has been shown to have a range of bond angles [27], which contributes to the broadness of the spectral features present in the experiment.

Figure 3 shows the experimental oxygen *K*-edge XANES spectra at various laser fluences, 2.5, 5.5, and 15 J/cm^2 corresponding to absorbed energy densities of 1.7, 3.8, and 10.5 MJ/kg. The optical x-ray time delay is integrated

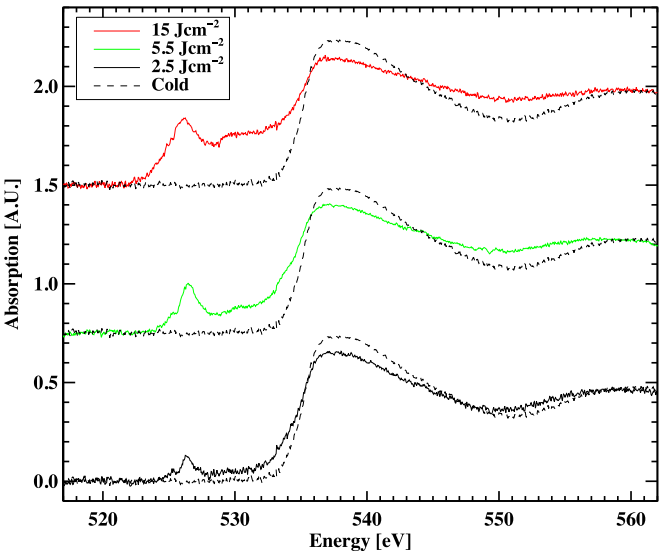

FIG. 3. (Color online) The experimental O 1s XANES spectra of SiO_2 at various laser fluences.

from 2 to 20 ps. In comparison with the room temperature XANES spectrum, four qualitative changes are observed. The absorption edge is broadened. There is reduced contrast above the edge. There is absorption within the band gap. Finally, a peak is seen below the band gap (9 eV below the edge).

As stated previously, the x-ray streak camera time resolution is much higher than 20 ps; however, only subtle changes in the spectra were observed within this range of time delay. Figure 4 shows the experimental oxygen K-edge XANES spectra at time delays −2, 0, 2, 4, 8, 14, and 20 ps for a fluence of 5.5 J/cm^2. Immediately following the laser pulse, the 2 ps spectrum exhibits the spectral features described above. Beyond 2 ps, the temporal evolution of the spectra

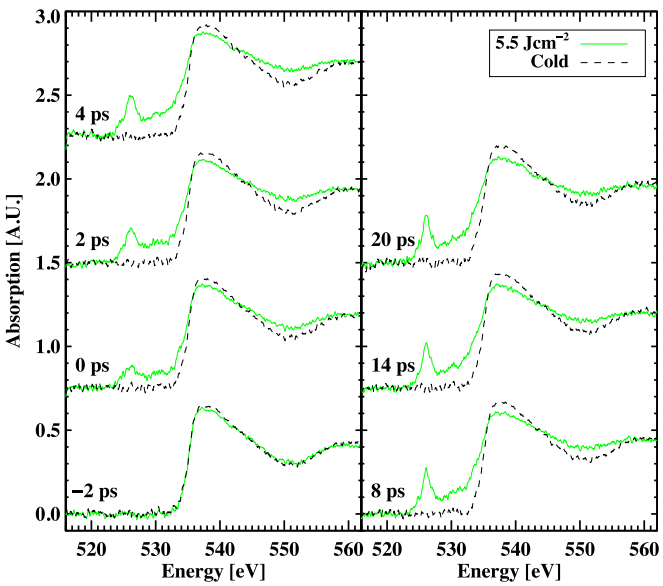

FIG. 4. (Color online) The experimental O 1s XANES spectra of SiO_2 at various time delays for a fluence of 5.5 J/cm^2. Each spectrum is generated by integrating over a 2 ps window that is centered at the stated time delay.

show a slight increase in the broadening of the edge and further reduction of the contrast above the edge.

In order to fully interpret the experimental spectra, we have performed *ab initio* MD simulations for SiO_2 at solid density (2.65 g/cc) and temperatures of 300, 5000, and 10 000 K using the ABINIT electronic structure code [28,29]. All calculations are carried out in the framework of the DFT with the generalized gradient approximation parametrization of the exchange and correlation [30]. The PAW (projector augmented wave) [31,32] atomic data for Si consists of four outer electrons ($3s^2 3p^2$) and a cutoff radius of $r_c = 1.7$ bohrs and six outer electrons ($2s^2 2p^4$) and a cutoff radius of $r_c = 1.2$ bohrs for O. We used an energy cutoff of 680 eV. To obtain silica structure at a given temperature, 36 Si and 72 O atoms initially arranged in the perfect quartz lattice were propagated up to 1 ps using time steps of 1 fs in the isokinetics ensemble. All MD calculations were performed at the Γ point. To obtain the optical response in the x-ray domain, we performed a detailed calculation of the electronic structure using a $3 \times 3 \times 3$ Monkhorst-Pack mesh and 2000 bands. Then we applied linear response theory to obtain XANES spectra extending 30 eV above the edge, following the method described in the references [33,34]. The XANES spectrum is obtained in the so-called impurity model, by considering the absorbing atom in an excited state. The PAW atomic data for the absorbing atom is generated by using a hole in the 1s orbital of O. This calculation provides a simple way for introducing the core electron-hole interaction in the independent-particle description used here [25]. For each ionic configuration, this impurity is moved onto several O atoms in the cell. Each completed spectrum is obtained by averaging the individual spectra obtained for different impurity positions in the ionic configurations.

The room temperature theoretical spectrum for α-quartz is displayed in Fig. 2(b). The calculated spectrum has been shifted in photon energy to match the position of the experimental absorption edge and convolved with the experimental resolution. There is satisfactory agreement both with the experiment and with previous calculated room temperature XANES spectra [24]. As previously noted by Taillefumier *et al.* [25], the calculated α-quartz spectral features are slightly contracted and the first maximum is narrower compared to measured amorphous SiO_2.

Figure 5 displays the calculated O 1s spectra for three electron temperatures, $T_i = T_e$, $T_e = 20\,000$ K, and $T_e = 30\,000$ K. In each case, spectra are shown for ion temperatures of 300, 5000, and 10 000 K. In the calculated spectra, the same qualitative changes are seen as in the laser heated spectra. As the ion temperature increases, the edge broadens, and the contrast above the edge is reduced. As the electron temperature increases, a peak forms below the band gap and absorption occurs within the band gap.

Figure 6 displays the radial distribution function $g(r)$ calculated for O-O, Si-O, and Si-Si, where the different curves show the equilibrium cases of equal T_e and T_i at 300, 5000, and 10 000 K. The height of the first peak in all three $g(r)$ curves is reduced dramatically at the elevated temperatures. For the Si-O $g(r)$, this change may be interpreted as a result of broken Si-O bonds. In the $g(r)$ for O-O at 10 000 K a small peak is observed at 1.4 Å, indicative of O atoms directly bonded to other O atoms. In general, the diminished structure in the $g(r)$

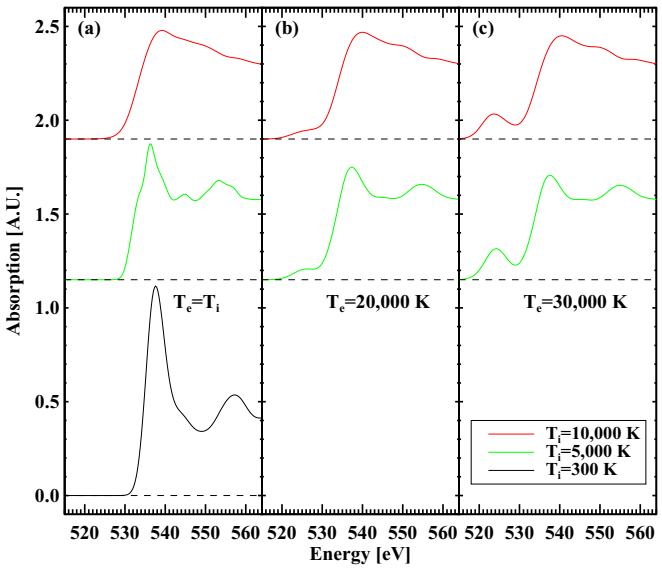

FIG. 5. (Color online) The calculated O 1*s* XANES spectra of SiO_2 at $T_i = 300$ (α-quartz), 5000, and 10 000 K (liquid), where $T_e = T_i$ in (a) at $T_e = 20\,000$ K in (b), and at $T_e = 30\,000$ K in (c).

reflects an increased disorder in the high temperature liquid SiO_2.

As previously pointed out in Mancic *et al.* [5] for the case of aluminum, the sharpness of the spectral features is correlated with the degree of local order. As the ionic temperature increases, the contrast of the minimum above the edge was reduced when the aluminum became a high temperature liquid. Similarly in the calculated SiO_2 XANES spectra, the

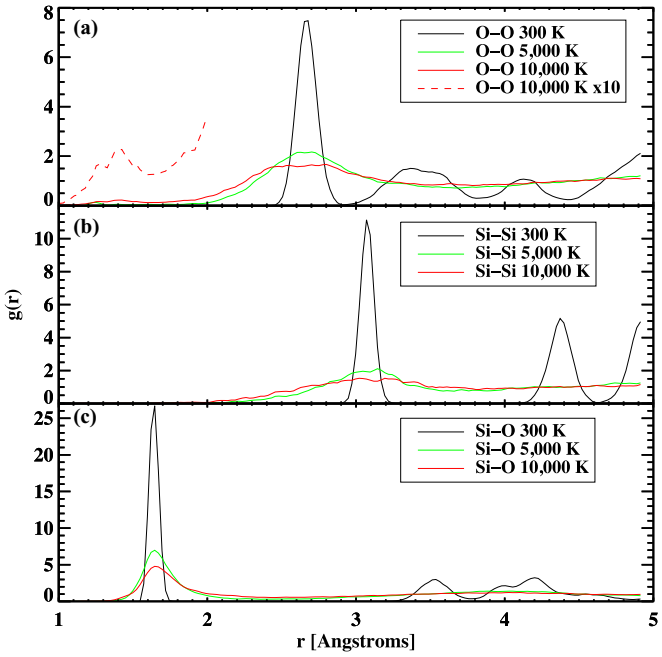

FIG. 6. (Color online) Radial distribution functions $g(r)$ for SiO_2 under the conditions of $T_e = T_i$ at 300, 5000, and 10 000 K for (a) O-O, (b) Si-Si, and (c) Si-O. The 10 000 K O-O $g(r)$ in (a) (red dashed line) has been multiplied by 10 to illuminate the peak at 1.4 Å.

absorption edge is broadened and the structure above the edge becomes less marked as the ion temperature increases. In the high temperature SiO_2 structure, there are broken silicon-oxygen tetrahedra, which can be seen in Fig. 6(c) from the decreased height of the first peak in the Si-O radial distribution function. The experimental spectra in Fig. 3 also show this behavior, with the slope of the edge and the contrast above the edge decreasing as the laser fluence increases. In addition, Fig. 4 shows a small reduction in the slope of the edge and the contrast above the edge with increasing time delay. This indicates an increase of the ion temperature with increasing laser fluence as well as some rise in the ion temperature in the first 20 ps following the laser pulse. The minimum above the edge is present in all of the experimental laser-heated spectra as well as in the calculated spectra at 300 and 5000 K, but missing in the calculation at 10 000 K. This comparison indicates that the experimental ion temperatures are less than 10 000 K.

Absorption within the band gap is seen in both the experimental laser heated in Fig. 3 and calculated XANES spectra at T_i of 5000 and 10 000 K. At low laser fluence, there is a small absorption in the band gap. At the higher fluences, this absorption increases. As the temperature increases, the band gap is filled with defect states originating from broken Si-O bonds [15]. This loss of bonding states in the electron structure is reflected in the ion structure by the reduced height of the first peak of $g(r)$ for Si-O. The observation of broken Si-O bonds and increased disorder indicate a possible mechanism for laser-induced optical damage as well as for laser writing of waveguides.

The effect of the electron temperature on the SiO_2 XANES spectra is now considered. The O 1*s* XANES spectra show the unoccupied *p*-like DOS. For quartz, the topmost valence band has been assigned to nonbonding oxygen 2*p* orbitals [35]. This band is occupied at room temperature and does not appear in the spectra. As electronic temperature increases, this band will start to be depopulated by the Fermi-Dirac function and appear in the XANES spectrum as a pre-edge peak. When the electronic temperature increases, the size of the pre-edge peak increases as the number of empty states rises. There is also a shift of the pre-edge peak to lower photon energy as states are depopulated further from the Fermi level. In both experimental and calculated spectra, this behavior is observed.

As the structure of SiO_2 is modified by the ultrafast laser pulse [14,15], it is important to consider if different O bonding geometries may contribute to the pre-edge feature. A pre-edge peak has been previously measured at 528.3 eV for vitreous silica and attributed to a π^* state from O-O bonding [36]. Here the pre-edge peak is seen at a different energy, 526 eV. Oxygen atoms in three-membered rings have been predicted [15], but the XANES spectral signature of these O atoms is not known. The calculated density of states below the Fermi level changes at the different temperatures: 300, 5000, and 10 000 K and may be effected by the presence of different oxygen structures.

Using a simple formulation for collisions, based upon a calculated electron-ion collision rate of 2.5 fs^{-1} [37,38], the equilibration time between the electron and ion temperature is estimated to be 43 ps. Following the formulation given by Lin *et al.* [11], the temperature dependent electronic heat capacity is calculated from the density of states and used to estimate T_e immediately after the laser excitation, giving $T_e = 20\,000$,

30 000, and 50 000 K for the three absorbed energy densities. For the measurement at 2–20 ps, the electron temperature may be higher than the ion one. The height of the pre-edge peak is a sensitive measure of the electronic temperature. The calculated absorption spectra show a defined pre-edge at $T_e = 30\,000$ K, which is not present at $T_e = 20\,000$ K. The calculation underestimates the band gap as 5.5 eV compared to the known value of 8.9 eV [18] because of a known limitation of DFT [35]. For this reason, a direct determination of T_e is omitted. Nonetheless, it is concluded that the warm dense SiO_2 formed by the ultrafast laser excitation is observed to be in a nonequilibrium state with $T_e > T_i$.

In conclusion, measurements and calculations have been performed of the XANES spectrum of warm dense SiO_2. The heated material is seen to have an electronic structure distinct from the room temperature solid. Through comparisons of measured and simulated spectra, the spectral features are understood and insight into both the local ionic and electronic behavior is gained. Following the laser excitation, Si-O bonds are broken, resulting in states within the band gap that increase with laser fluence. Spectral features constrain the ionic temperature, while a peak below the band gap shows unoccupied states in the valence bands consistent with a high electronic temperature, indicating the presence of a nonequilibrium liquid with $T_e > T_i$. A reduced sharpness of spectral features reflects an increased disorder in this high temperature liquid. These XANES measurements provide a detailed description of how SiO_2 transforms from an insulator with well-defined local structure to a high temperature liquid with reduced Si-O bonding.

The authors thank Patrick Renaudin for illuminating discussions. This work was performed at LBNL under the auspices of the U.S. Department of Energy, Office of Science, Basic Energy Sciences, Materials Sciences Division Contract No. DE-AC02-05CH11231. This material is based upon work supported at UC Berkeley by the U.S. Department of Energy, Office of Science, Office of Fusion Energy Sciences and by the National Nuclear Security Administration under Awards No. DE-FG52-10NA29649 and No. DE-NA0001859.

[1] R. W. Lee, H. A. Baldis, R. C. Cauble, O. L. Landen, J. S. Wark, A. Ng, S. J. Rose, C. Lewis, D. Riley, J.-C. Gauthier, and P. Audebert, Laser Part. Beams **20**, 527 (2002).
[2] M. Ross, Nature (London) **292**, 435 (1981).
[3] M. Koenig, A. Benuzzi, B. Faral, J. Krishnan, J. M. Boudenne, T. Jalinaud, C. Rémond, A. Decoster, D. Batani, D. Beretta, and T. A. Hall, Appl. Phys. Lett. **72**, 1033 (1998).
[4] J. W. Chan, T. Huser, S. Risbud, and D. M. Krol, Opt. Lett. **26**, 1726 (2001).
[5] A. Mančić, A. Lévy, M. Harmand, M. Nakatsutsumi, P. Antici, P. Audebert, P. Combis, S. Fourmaux, S. Mazevet, O. Peyrusse, V. Recoules, P. Renaudin, J. Robiche, F. Dorchies, and J. Fuchs, Phys. Rev. Lett. **104**, 035002 (2010).
[6] A. Benuzzi-Mounaix, F. Dorchies, V. Recoules, F. Festa, O. Peyrusse, A. Lévy, A. Ravasio, T. Hall, M. Koenig, N. Amadou, E. Brambrink, and S. Mazevet, Phys. Rev. Lett. **107**, 165006 (2011).
[7] P. M. Leguay, A. Lévy, B. Chimier, F. Deneuville, D. Descamps, C. Fourment, C. Goyon, S. Hulin, S. Petit, O. Peyrusse, J. J. Santos, P. Combis, B. Holst, V. Recoules, P. Renaudin, L. Videau, and F. Dorchies, Phys. Rev. Lett. **111**, 245004 (2013).
[8] S. Mazevet, V. Recoules, J. Bouchet, F. Guyot, M. Harmand, A. Ravasio, and A. Benuzzi-Mounaix, Phys. Rev. B **89**, 100103 (2014).
[9] C. Marini, F. Occelli, O. Mathon, R. Torchio, V. Recoules, S. Pascarelli, and P. Loubeyre, J. Appl. Phys. **115**, 093513 (2014).
[10] B. I. Cho, K. Engelhorn, A. A. Correa, T. Ogitsu, C. P. Weber, H. J. Lee, J. Feng, P. A. Ni, Y. Ping, A. J. Nelson, D. Prendergast, R. W. Lee, R. W. Falcone, and P. A. Heimann, Phys. Rev. Lett. **106**, 167601 (2011).
[11] Z. Lin, L. V. Zhigilei, and V. Celli, Phys. Rev. B **77**, 075133 (2008).
[12] T. G. White, J. Vorberger, C. R. D. Brown, B. J. B. Crowley, P. Davis, S. H. Glenzer, J. W. O. Harris, D. C. Hochhaus, S. Le Pape, T. Ma, C. D. Murphy, P. Neumayer, L. K. Pattison, S. Richardson, D. O. Gericke, and G. Gregori, Sci. Rep. **2**, 889 (2012).
[13] P. Celliers, A. Ng, G. Xu, and A. Forsman, Phys. Rev. Lett. **68**, 2305 (1992).
[14] N. Fukata, Y. Yamamoto, K. Murakami, M. Hase, and M. Kitajima, Appl. Phys. Lett. **83**, 3495 (2003).
[15] M. Boero, A. Oshiyama, P. L. Silvestrelli, and K. Murakami, Physica B **376**, 945 (2006).
[16] A. Denoeud, A. Benuzzi-Mounaix, A. Ravasio, F. Dorchies, P. M. Leguay, J. Gaudin, F. Guyot, E. Brambrink, M. Koenig, S. Le Pape, and S. Mazevet, Phys. Rev. Lett. **113**, 116404 (2014).
[17] O. Anderson and C. Ottermann, in *Thin Films on Glass*, edited by H. Bach and D. Krause (Springer, Berlin, 1997), pp. 165–167.
[18] B. El-Kareh, *Fundamentals of Semiconductor Processing Technologies* (Kluwer Academic, Norwell, MA, 1995).
[19] L. Martin-Samos, G. Bussi, A. Ruini, E. Molinari, and M. J. Caldas, Phys. Rev. B **81**, 081202 (2010).
[20] B. C. Stuart, M. D. Feit, A. M. Rubenchik, B. W. Shore, and M. D. Perry, Phys. Rev. Lett. **74**, 2248 (1995).
[21] P. A. Heimann, T. E. Glover, D. Plate, H. J. Lee, V. C. Brown, H. A. Padmore, and R. W. Schoenlein, in *Ninth International Conference on Synchrotron Radiation Instrumentation*, edited by J.-Y. Choi and S. Rah, AIP Conf. Proc. No. 879 (AIP, New York, 2007), p. 1195.
[22] J. Feng, K. Engelhorn, B. I. Cho, H. J. Lee, M. Greaves, C. P. Weber, R. W. Falcone, H. A. Padmore, and P. A. Heimann, Appl. Phys. Lett. **96**, 134102 (2010).
[23] B. T. Poe, C. Romano, and G. Henderson, J. Non-Cryst. Solids **341**, 162 (2004).
[24] Z. Wu, F. Seifert, B. Poe, and T. Sharp, J. Phys.: Condens. Matter **8**, 3323 (1999).
[25] M. Taillefumier, D. Cabaret, A.-M. Flank, and F. Mauri, Phys. Rev. B **66**, 195107 (2002).
[26] I. Davoli, E. Paris, S. Stizza, M. Benfatto, M. Fanfoni, A. Gargano, A. Bianconi, and F. Seifert, Phys. Chem. Miner. **19**, 171 (1992).
[27] F. Liebau, *Structural Chemistry of Silicates* (Springer, Berlin, 1985).

[28] X. Gonze, B. Amadon, P. M. Anglade, J. M. Beuken, F. Bottin, P. Boulanger, F. Bruneval, D. Caliste, R. Caracas, M. Côté, T. Deutsch, L. Genovese, P. Ghosez, M. Giantomassi, S. Goedecker, D. R. Hamann, P. Hermet, F. Jollet, G. Jomard, S. Leroux, M. Mancini, S. Mazevet, M. J. T. Oliveira, G. Onida, Y. Pouillon, T. Rangel, G. M. Rignanese, D. Sangalli, R. Shaltaf, M. Torrent, M. J. Verstraete, G. Zerah, and J. W. Zwanziger, Comput. Phys. Commun. **180**, 2582 (2009).

[29] F. Bottin, S. Leroux, A. Knyazev, and G. Zérah, Comput. Mater. Sci. **42**, 329 (2008).

[30] J. P. Perdew, K. Burke, and M. Ernzerhof, Phys. Rev. Lett. **77**, 3865 (1996).

[31] M. Torrent, F. Jollet, F. Bottin, G. Zérah, and X. Gonze, Comput. Mater. Sci. **42**, 337 (2008).

[32] P. E. Blöchl, Phys. Rev. B **50**, 17953 (1994).

[33] V. Recoules and S. Mazevet, Phys. Rev. B **80**, 064110 (2009).

[34] S. Mazevet, M. Torrent, V. Recoules, and F. Jollet, High Energy Density Phys. **6**, 84 (2010).

[35] G. Kresse, M. Marsman, L. E. Hintzsche, and E. Flage-Larsen, Phys. Rev. B **85**, 045205 (2012).

[36] N. Jiang and J.C. Spence, Ultramicroscopy **106**, 215 (2006).

[37] P. Martin, S. Guizard, P. Daguzan, G. Petite, P. D'Oliveira, P. Meynadier, and M. Perdrix, Phys. Rev. B **55**, 5799 (1997).

[38] D. Arnold, E. Cartier, and D. J. DiMaria, Phys. Rev. B **45**, 1477 (1992).